

University of New Hampshire

University of New Hampshire Scholars' Repository

Honors Theses and Capstones

Student Scholarship

Spring 2023

Low Frequency Waves Due to He⁺ as Observed by the Ulysses Spacecraft

Anastasia V. Marchuk

University of New Hampshire, Durham

Follow this and additional works at: <https://scholars.unh.edu/honors>



Part of the [Physics Commons](#)

Comments

A summary of this thesis was translated into Russian as a part of a major in Russian, and can be found at the end of the document before the references.

Recommended Citation

Marchuk, Anastasia V., "Low Frequency Waves Due to He⁺ as Observed by the Ulysses Spacecraft" (2023). *Honors Theses and Capstones*. 774.

<https://scholars.unh.edu/honors/774>

This Senior Honors Thesis is brought to you for free and open access by the Student Scholarship at University of New Hampshire Scholars' Repository. It has been accepted for inclusion in Honors Theses and Capstones by an authorized administrator of University of New Hampshire Scholars' Repository. For more information, please contact Scholarly.Communication@unh.edu.

Low Frequency Waves Due to He^+ as Observed by the Ulysses Spacecraft

Anastasia Marchuk

Physics Department and Space Science Center, Morse Hall, University of New Hampshire, Durham, New Hampshire, USA

May 15, 2023

Abstract

We surveyed magnetic field data from the Ulysses spacecraft and found examples of magnetic waves with characteristics that point to excitation by newborn pickup He^+ . With interstellar neutrals as the likely source for the pickup ions, we have modeled the ion production rates and used them to produce wave excitation rates that we compare to the background turbulence rates. The source ions are thought to be always present, but the waves are seen when growth rates are comparable to or exceed the turbulence rates. With the exception of the fast latitude scans, and unlike the waves excited by newborn interstellar pickup H^+ , the waves are seen throughout the Ulysses orbit.

1 Introduction

A question that plagues a lot of scientific research, especially of the sort that an undergraduate is qualified enough to help with, seems very simple on the surface. "What's the point of your research?" I can answer this question in a couple different ways. The simplest response for me is, "to look for these waves." But this inevitably brings the follow up question of, "but why are people looking for these waves?" My go to answer has been, for a long time, "because we want to know if they're there or not." This is also true, on the surface. We know that waves are generated by pickup ions, and different kinds of ions make waves at different frequencies. Before the Ulysses mission, we already knew about pickup ion waves, but we had not sent a spacecraft on the unique trajectory that Ulysses took. My work and the work of plenty of other researchers before me looked first at all the data from Ulysses, learning a lot about the solar wind, the activity of the Sun and how it changes from solar minimum to solar maximum, and then at signatures in the data like pickup ion waves. We found a few H^+ waves, then a lot more, then a few He^+ waves, and then I sat down and found, well, a lot of them! However, perhaps understandably, the answers I usually give to

these questions are not very satisfying. I understand that - physics research sounds a bit inherently glamorous, and to find out that we look for waves because we think there might be waves and we want to be sure if they exist or not can be a bit of a let-down, however well meaning one might be.

We can dig a little bit deeper than this for much better results. We do, of course, want to know if the waves are there or not, but what we really want to do is understand what our solar system does and how it works. Let's do that with this work - we know that the heliosphere is like a huge balloon, inflated by the solar wind. The heliosphere is the protective barrier for the solar system, and it keeps out everything it can see - anything that can interact with a magnetic field. That means that neutral particles, like hydrogen and helium atoms, can get inside. These atoms get ionized, start interacting with the Sun's magnetic field, and generate low-frequency magnetic waves. They are, in a sense, picked up by the solar wind and the Sun's magnetic field, earning them the name pickup ions (PUIs). When we started learning about the solar wind, we found that it began very hot and cooled as it flowed away from the sun. We know how this cooling, called adiabatic cooling, works - when a hot gas expands, it cools down. But far away from the Sun, beyond 10 AU, the solar wind was warmer than it should be, and we didn't know why. Now, the leading theory is that the wave energy from those pickup ions is dissipated by turbulence in interplanetary space, and that energy goes on to heat the background plasma. This work operates on that assumption. In finding the distribution of pickup ion wave observation, we learn more about wave excitation rates, ion distribution, and turbulence, and we also found high frequency waves that we don't yet understand.

This work, and the research I and many others do, expands our knowledge of the dynamics of local interplanetary space in our own solar system. Shedding light on one small mystery adds to our comprehensive understanding of interplanetary dynamics. It's where we live - we ought to figure out how it works here. As we learn about our own solar system, we can apply that understanding to other planetary systems, too.

2 Solar Wind

To discuss pickup ions, we first need to understand the solar wind, and to understand that, we need to look at the Sun. The Sun's outer layer of atmosphere, the corona, does not have a defined "edge" in the way the Earth's atmosphere does. This is most noticeable in diagrams and images, like Figure 1, that show large wispy structures extending far from the surface in some places, and seemingly empty space in others. Their size, location, and intensity changes constantly, as the Sun's activity changes from solar minimum to solar maximum. While the Earth's atmosphere ends at the boundary between Earth's terrestrial radiation and solar radiation from space, no such boundary exists for the Sun. In fact, there is no way to distinguish a boundary between the edge of the corona and the beginning of open space in the solar system. The wispy structures fade from view, but the only boundary we

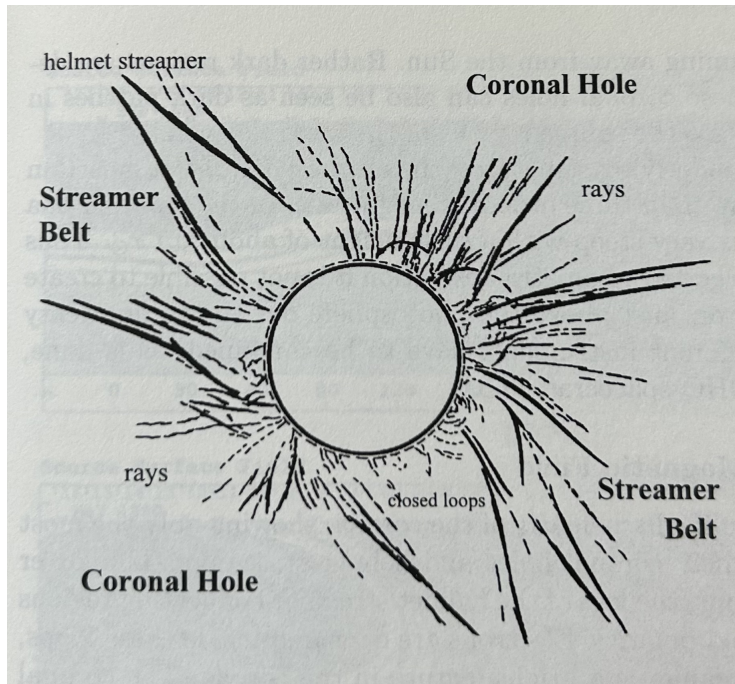


Figure 1: Coronal structure during the total eclipse of 11 July 1991. Based on a sketch by S. Koutchmy n K. Lang [8.53], *Sun, earth and sky*, Copyright 1995, Springer Verlag (Figure and caption reproduced from Space Physics by MB Kallenrode)

can really identify for the atmosphere of the Sun is at the edge of the heliosphere - a bubble in the greater interstellar medium that contains our entire Solar system and is sustained by the solar wind and the Sun's magnetic field. The wind speed is essentially constant all the way to the termination shock, and the density decreases as R^{-2} .

The Sun is constantly emitting electrically charged particles in every direction, with protons and electrons constituting the bulk of the population. This is the solar wind. The speed of solar wind and its other features depend on the structure visible in the corona. The fast solar wind comes from the dark, seemingly empty areas of the corona, aptly named coronal holes. The locations of the coronal holes vary from solar minimum to solar maximum. The slow solar wind comes from an area near the streamer belt, a region near the Sun's equator, full of those wispy structures that are called coronal or helmet streamers. The slow solar wind streams at a speed of 250 to 400 km/s, whereas the fast solar wind can be 400 to 800 km/s. It blows away the edges of the corona out into the heliosphere. Ionization of neutral hydrogen is based on the flux of solar wind protons.

The magnetic field of the Sun is complex, especially within a few solar radii of the surface. However, for our purposes, we can safely ignore all of that and look at the larger

field structure. The solar wind expands outward radially from the Sun, and the Sun's magnetic field is frozen-in. A magnetic field can be frozen into a plasma because the charged particles conduct electricity and influence the field, and the field in turn influences the charged particles, forcing them to always act together. As the wind flows outward it carries the magnetic field into the heliosphere, but while the wind moves out, the lines move west due to the combined forces of the rotation of the Sun and the radial solar wind expansion. The Sun rotates with a period of about 27 days. Since the solar wind moves outward, but the magnetic field lines move westward, the field winds up and creates a spiral shape known as the Parker spiral. This spiral shape is wavy because the rotation axis of the Sun and the axis of the magnetic dipole of the Sun are not aligned. The barrier where top and bottom halves meet, so to speak, is called the heliospheric current sheet. This is the wavy ballerina skirt shape depicted in Figure 2. The northern half is either positively or negatively polarized, while the southern is the opposite - field lines on one side point towards the Sun, while those on the other side point away from the Sun. The magnetic field of the Sun reverses every 11 years.

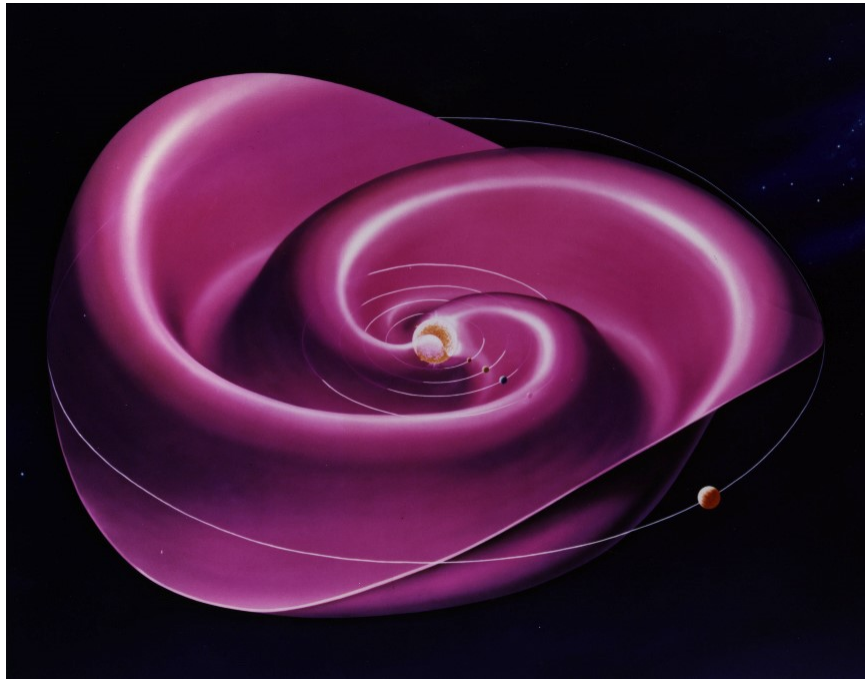


Figure 2: "An artist's concept of the heliospheric current sheet. The rotating Sun is located in the center. The current sheet circles the Sun's equator like a wavy skirt around a ballerina's waist." First published in Wilcox et al. (1980). It was drawn by Werner Heil, NASA artists, developed by Prof. John Wilcox.

The current sheet is the largest structure in the entire heliosphere. As you might

imagine, it plays a role in interplanetary space, but not so much that it heavily impacts the dynamics described here. There are complex interacting flows in the wind that we will also avoid - shocks, stream interfaces, etc. What is important is that for our purposes, the solar wind overall is collisionless with a neutral charge density. This means that it is safe to assume that for the most part, particles of the solar wind do not hit each other, and that there are an approximately equal number of positively and negatively charged particles in any given volume.

3 Pickup Ions and Interstellar Neutrals

The waves we study are inside the heliosphere, so it's important to understand the interaction between interstellar particles and the heliosphere. Neutrals can pass into the heliosphere, and there are more or less neutrals of different species in different areas depending on many different factors. Once a neutral gets ionized, it is picked up and flows along the magnetic field. When the ions are resonant with other waves, they scatter, creating the low frequency magnetic waves we study.

3.1 The Heliosphere

The heliosphere is the part of the universe under the influence of the Sun, as shown in an artist's representation in Figure 3. The edge of the heliosphere, where the solar wind and the Sun's magnetic field lines meet the interstellar medium, is called the termination shock. The heliosheath is the zone beyond that, where the solar winds are in equilibrium with the wind of the interstellar medium, and the heliopause is the boundary at the edge where solar wind plasma cannot penetrate any further. Beyond this is theorized to be the bow shock, a feature that might exist in front of the heliosphere as a result of the forward motion of the system. The closest that interstellar plasma can get to our Solar System is the termination shock, so called because at that boundary the solar wind speed drops abruptly. The heliosphere as a whole can be thought of as the Solar System's protective bubble, keeping out the interstellar medium as the Solar System moves through it at 25k km/s. However, this is not strictly true. While the magnetic field and the charged particles of the solar wind prevent most interstellar charged particles from entering the Solar System, neutral particles cannot interact with charged particles or a magnetic field, and so pass easily through the termination shock and into the heliosphere. High energy cosmic rays are strong enough to pass through as well.

3.2 From Neutrals to Ions

These interstellar neutral particles, once inside the heliosphere, are unlikely to remain neutral forever. Often they are ionized one of two ways. The primary means of producing pickup ions is through collision with a charged particle from the solar wind. The primary

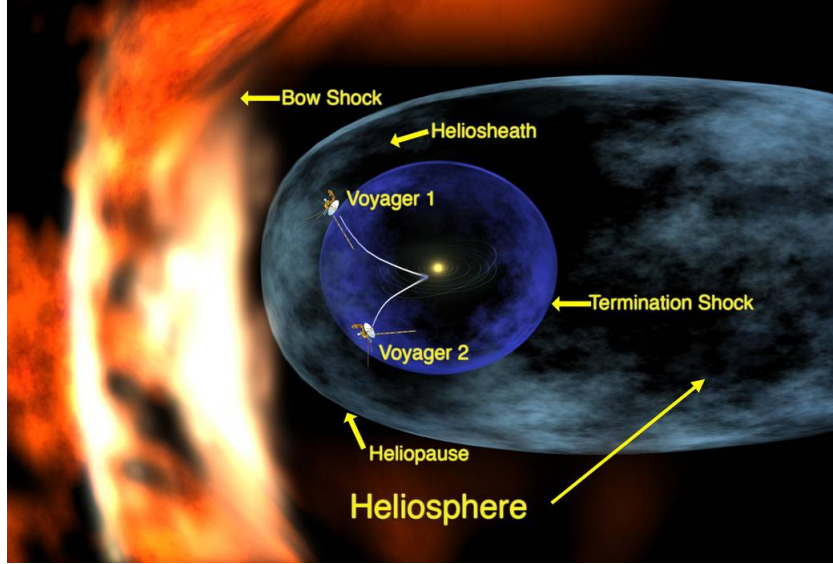


Figure 3: A diagram of the heliosphere, labeling the termination shock, heliosheath, heliopause, and theorized bow shock as well as the current locations of the Voyager missions. Image Credit: NASA/Goddard/Walt Feimer

means of producing pickup H^+ is through collision of a neutral interstellar H atom with a charged particle from the solar wind. The interaction between the solar wind proton and the neutral can cause a charge exchange, ionizing the neutral and neutralizing the proton, or the electron can be lost without charge exchange. Alternatively, an extreme ultraviolet (EUV) solar photon can ionize an interstellar neutral. If the energy of the photon and the binding energy of an electron in the neutral are the same, this collision can cause an electron to be ejected from the neutral, which ionizes it. This is the primary mechanism for making He^+ ions from neutral helium [Sokół et al.(2020)]. Once these particles are charged, they begin to interact with the magnetic field. Nearly stationary before, they now flow at the solar wind speed. In other words, they are "picked up" by the solar wind, hence the name pickup ions. Due to the Lorentz force, these ions begin to orbit the field in a circular motion. The ion's cyclotron frequency is the frequency of this orbit. Once this atom is ionized, it immediately accelerates, as it is now under the control of the magnetic field.

3.3 Neutral and PUI Distribution

The distribution of interstellar neutrals and PUIs can affect where we see wave events. Different areas of the heliosphere have more or less hydrogen and helium in various states. Zank (2016) describes three distinct regions of the local interstellar medium and heliosphere that are the source of unique neutral hydrogen sources. As pictured in Figure 4, Region

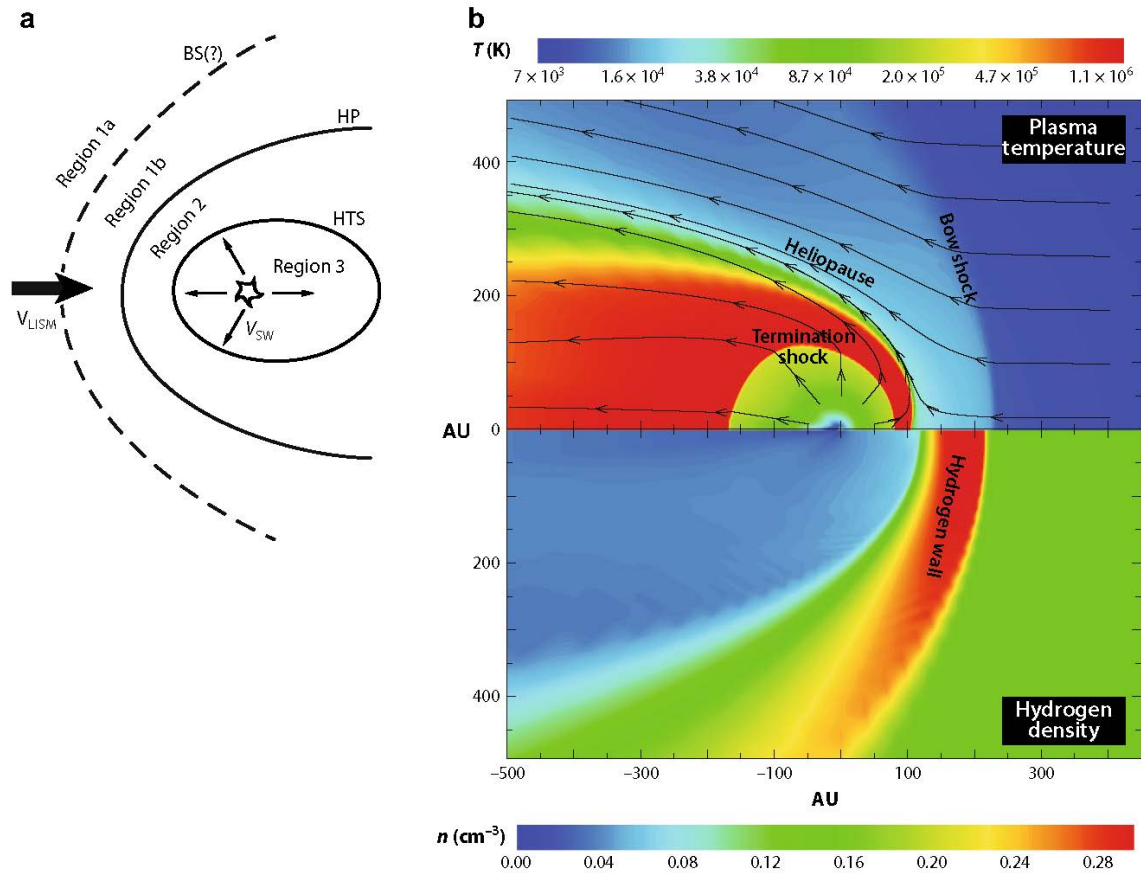


Figure 4: A diagram of the heliosphere. Left: diagram of the solar wind-VLISM (very local interstellar medium) boundary regions which are thermodynamically distinct. HTS is heliospheric termination shock, HP is heliopause, BS is bow shock, VSW denotes the radial solar wind flow speed, and VLISM the LISM flow velocity. Right: top half: logarithmic temperature distribution of the interstellar plasma and solar wind, and bottom half: density distribution of neutral hydrogen. This figure reproduced from Zank (2016).

1 is split into 1a and 1b: 1a is the area beyond the bow shock, and 1b is between the heliopause and the bow shock. The plasma flow speed and temperature are lower, but the density is higher there than in the other regions. Region 2 is beyond the heliopause, in the heliosheath. This is right outside the termination shock, where the solar wind has just slowed down to subsonic speeds and in doing so become very hot. Density is high here as well, with large magnetic fields, but the wind speed is much lower than the next region. Region 3 is inside the termination shock, where we are, and where the solar wind is supersonic. The temperature and densities are low here compared to the other regions.

The right side of the plot shows plasma temperatures, which demonstrates the high temperature of the heliosheath region, but more interestingly shows the hydrogen density in each region. A noticeable feature is the hydrogen wall right behind the bow shock - a large population of neutral hydrogen. PUIs can be made in all three regions. In Region 3, ionization occurs through some type of collision or charge exchange, or by collision with an EUV photon. In Region 2, they are either interstellar neutrals that experience charge exchange, or PUIs created in Region 3 that crossed the termination shock and entered the heliosheath. In Region 3, the area we study (inside the termination shock), H^+ PUIs are not found within 3AU of the Sun.

There is another interesting feature in the distribution of helium in the heliosphere. Gloeckler et al. (2004) describes the gravitational focusing cone of helium behind the Sun. In this context, in front of the Sun would be towards the direction of the bow shock and interstellar medium, and behind the Sun would be the farther side, downstream. The Sun's gravity pulls in heavier interstellar neutrals into this cone shaped region. Since hydrogen and therefore H^+ PUIs do not penetrate very close to the Sun, but helium can and does [Argall et al.(2015), Fisher et al.(2016), Hollick et al.(2018a)], He^+ PUIs are found not only close to the Sun but particularly in this focusing cone region with a high helium density.

Figure 5 shows traversals of the focusing cone by ACE, AMPTE, and Nozomi. Earth passes through the focusing cone every year in December. The reasons for the variability in size of the focusing cone are not yet understood. However, detecting pickup ions present in the focusing cone is very useful for measuring the size and other physical properties of the cone.

4 Wave Excitation

Pickup ions stream through the solar wind, and their motion lies well outside the thermal population. In the language of plasma instabilities, they constitute a "free energy" source that excites magnetic waves. It is very easy for this wave energy to be dispersed by background turbulence. When the turbulence is strong, it completely absorbs the wave energy. This energy is transported to smaller scales. Beyond about 10 AU, waves excited by interstellar PUIs provide the dominant energy source that drives the turbulence and heats the background plasma [Zank et al.(1996), Smith et al.(2001), Smith et al.(2006a), Pine

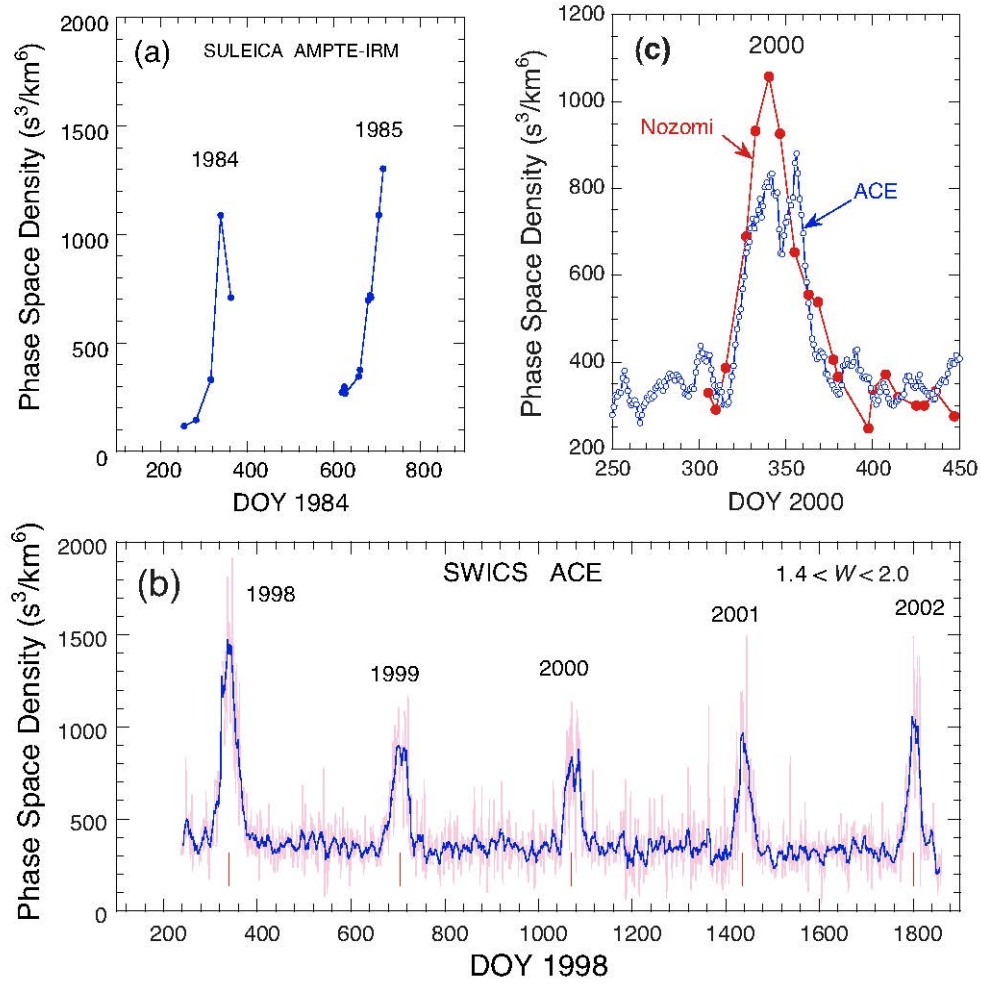


Figure 5: Crossings of the gravitational focusing cone of interstellar helium in 1984, 1985, and 1998-2002. Observations were made with AMPTE SULEICA, ACE SWICS, and Nozomi from different locations. This plot reproduced from Gloeckler et al. (2004).

et al.(2020)]. However, when the turbulence is low enough such that the wave energy can accumulate, that energy reaches an observable level and can be measured. It takes hours for the wave energy from scattered ions to accumulate, much longer than the time it takes to scatter an individual ion.

4.1 The Theory of Wave Excitation

These newly ionized pickup ions create the low frequency waves we study. They stream along the magnetic field towards the Sun. The velocity of ions is usually rendered in terms of velocity parallel to the magnetic field and velocity perpendicular to the magnetic field, which allows us to more specifically explain their motion. When the pickup ions are resonant with other MHD waves propagating parallel to the field, they can scatter - this is the cyclotron resonant instability which is stated to generate waves in Marchuk et al.(2021). Lee & Ip (1987) describes how the pickup ions distribute themselves into a ring-beam distribution in that parallel/perpendicular velocity space - basically a circle in $V_{parallel}$ and V_{perp} [Williams & Zank (1994), Zank 1999]. This distribution makes them vulnerable to instabilities and allows wave generation. They derive a formula for the time-asymptotic wave spectrum that assumes the particles have scattered completely. This avoids a situation where all particles enter at once and create distortions in the spectrum. Particles can accelerate off shocks, producing higher-energy particles that excite lower frequency waves that are not seen with pickup ions unless they, too, are accelerated by the same processes. This is why in order to properly simulate wave energy accumulation, we assume the contributing particles have already completely scattered and slowly iterate through the prediction. This is the basis of our wave excitation calculations.

Textbook wave examples have high ellipticity and are left-hand polarized in the spacecraft frame with a growth rate greater than the turbulence rate, propagating towards the sun. Since turbulence absorbs wave energy, an interval with low growth rate will not exhibit any wave traits. In studies with H^+ [Murphy et al.(1995), Cannon et al.(2013), Cannon et al.(2014a), Cannon et al.(2014b), Cannon et al.(2017)], the majority of events were at an ellipticity greater than 0.35, either positive or negative. In the past we excluded any events with an ellipticity lower than ± 0.35 because we wanted to be more conservative, but since we saw them here in greater abundance we want to address them as well. Removing these events did not preferentially remove them from any section of the orbit either. Figure 6 shows the location of the wave events along the orbit, with the bottom panel showing all events with $|Elip| > 0.35$.

4.2 Excitation Rates and Calculations

Waves are being excited all the time by the scattering of pickup ions. However, when the turbulence rate is higher than the rate of wave growth, it dissipates the wave energy rendering any waves unobservable. We are postulating that the long, slow accumulation of

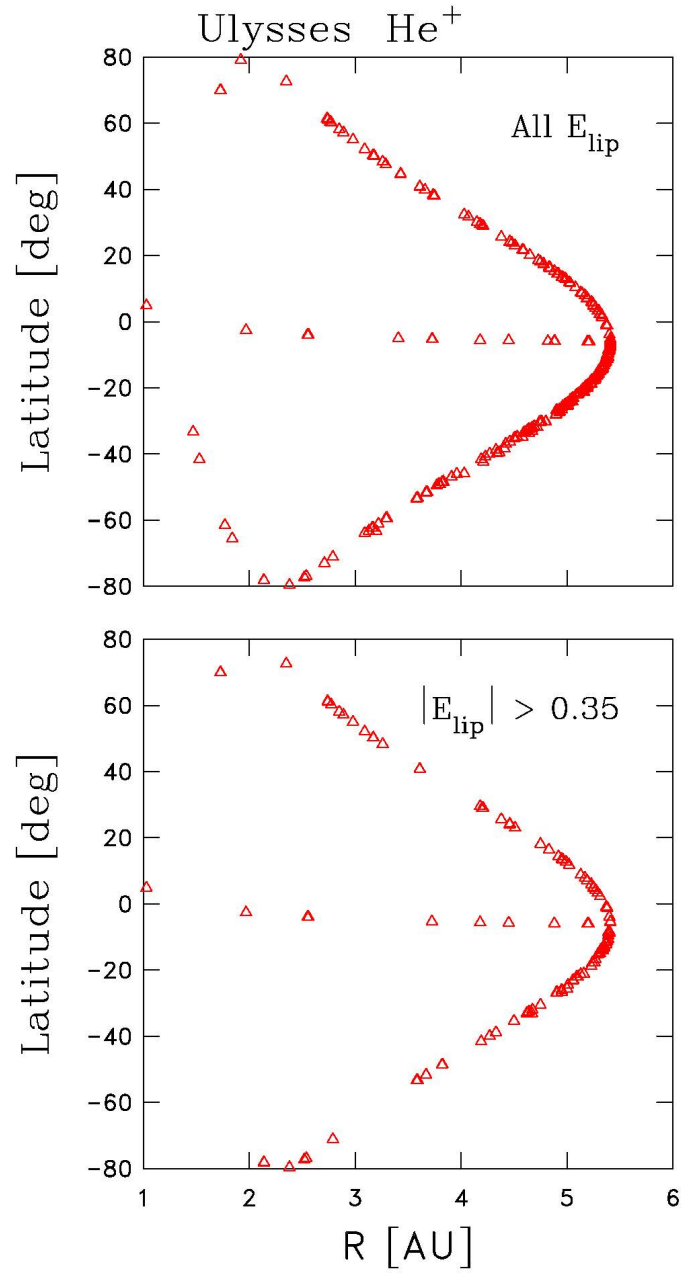


Figure 6: Location of He^+ excited wave events along the Ulysses trajectory. (top) Location of all intervals that are identified as He^+ events. (bottom) Location of all identified He^+ with $|E_{lip}| > 0.35$. This plot reproduced from Marchuk et al. (2021).

wave energy from scattered ions passes through a sequence of quasi-stationary, asymptotic states as predicted by Lee & Ip (1987). Below is described Lee & Ip's formula for the wave spectrum, and its associated wave enhancement term.

Lee & Ip's formula for the wave spectrum is given by

$$I_{\pm}(k, \infty) = \frac{1}{2} [C(k)^2 + 4I_+(k, 0)I_-(k, 0)]^{1/2} \pm \frac{1}{2}C(k), \quad (1)$$

in which at time equals zero, the background spectrum at wavenumber k for fluctuations is $I_+(k, 0)$ when propagating away from the Sun, and $I_-(k, 0)$ when propagating towards the Sun. The whole spectrum can be calculated by summing the four permutations of eq. 1 (i.e., $I_{tot}(k, \infty) = I_+(+k, \infty) + I_+(-k, \infty) + I_-(+k, \infty) + I_-(-k, \infty)$). Negative k represents right-hand polarized fast-mode waves, and positive k represents left-hand polarized Alfvén waves for waves moving sunward.

Clockwise rotation is right hand polarized, and counterclockwise left-hand polarized, when looking along the mean magnetic field. Fast mode, or fast magnetosonic waves, have a nonzero component along the mean magnetic field proportional to the density compression of the wave when propagating at oblique angles to the field. Alfvén waves have magnetic fluctuations that are perpendicular to both the direction of propagation and the mean magnetic field. So really, the only difference is the polarization in this case. This is strictly a one-dimensional theory that assumes waves propagating parallel and anti-parallel to the mean magnetic field with no oblique propagation.

The wave enhancement term $C(k)$ from eq. 1 describes the wave, and can be written as

$$C(k) = I_+(k, 0) - I_-(k, 0) + 2\pi m_i n_i V_A |\Omega_{i,c}| k^{-2} \left[\Omega_{i,c} k^{-1} v_0^{-1} - \frac{(\Omega_{i,c} k^{-1} v_0^{-1} - \mu_0)}{|\Omega_{i,c} k^{-1} v_0^{-1} - \mu_0|} \right], \quad (2)$$

where m_i is the pickup ion mass, n_i is the pickup ion number density, V_A is the Alfvén speed, v_0 is the PUI speed in the plasma frame, μ_0 is the pitch angle of the new pickup ions, v_0 is taken to be equal to the solar wind speed V_{SW} , and $\Omega_{i,c} = 2\pi f_{i,c}$ in which the ion cyclotron frequency is $f_{i,c} = e_i B / (2\pi m_i c)$. In that term, e_i is the charge of the pickup ion, B is the local magnetic field intensity, and c is the speed of light.

We assume that we can describe the background turbulent spectrum in eq. 2 with the equation $I_+(k, 0) = I_-(k, 0) = (1/4)I_{tot}(k_{i,c}, 0)k^{-5/3}$. The total background intensity at the ion cyclotron frequency in this equation is $I_{tot}(k_{i,c}, 0) = I_+(+k_{i,c}, 0) + I_-(-k_{i,c}, 0) + I_+(-k_{i,c}, 0) + I_-(+k_{i,c}, 0)$. This assumption is based on techniques from Joyce (2010) and first used in Cannon (2014b).

We can use these formulas to evaluate wave energy growth as the density of PUIs increases. To do this, we need to assume that the rate at which PUIs are produced is slow compared to the rate at which they are scattered, so that the wave spectrum passes through a series of asymptotic forms while the PUI density increases. We do this by using the computed PUI production rate and varying the accumulation time until it fits the power

level of the observed waves. That total wave power is computed at the peak of the spectrum associated with wave excitation. We do this for two different times near the fit time, using the differential to determine the rate of wave growth. Energy in the wave spectrum is created by ion cyclotron resonance with the population of PUIs. The rate at which this accumulates is given by

$$\frac{dE_W}{dt} = R_{ac} \times 10^{10} \times 10^{-5} \left(\frac{2\pi f_w}{V_{SW}} \right) \left(\frac{21.8^2}{N_P} \right) \cdot \frac{1}{3600}. \quad (3)$$

The factor 21.8 converts the magnetic field to Alfvén units, 10^{10} converts Gauss² to nT², and 10^{-5} converts cm to km. The solar wind speed V_{SW} is in km s⁻¹, and N_P is in cm⁻³. The spacecraft-frame frequency, where the wave power peaks, is f_w . The accumulation rate R_{ac} is given by $[I_{peak}(t_{acc2}) - I_{peak}(t_{acc1})]/[t_{acc2} - t_{acc1}]$. The two times in the accumulation rate, t_{acc2} and t_{acc1} , are used to find that differential. $I_{peak}(t_{acc})$ is $I_{tot}(k, \infty)$ evaluated at the peak of the wave enhancement using n_i equal to t_{acc} times the newborn PUI production rate.

The minimum acceleration that will readily produce a wave enhancement in the computed spectrum is t_{acc1} , and $t_{acc2} = t_{acc1} + 20$ hrs - the local maximum. Values other than 20 hrs only make the computed growth rates vary by $\sim 20\%$, with a couple varying by a factor of 2, but these variations are not significant enough to actually alter any conclusions. This is a prescription for using the above formalism to compute energy growth rates, but it is the comparison with the turbulence rate that decides if the wave is observable.

The time limit on accumulation comes in because waves need to be generated before the turbulent cascade destroys wave energy. According to Joyce (2011), the proton peak from H⁺ is about 17.3 hours and the helium peak from He⁺ is about 22.3 hours. Since these times are shorter than the time turbulence takes to transport that amount of energy through the wave frequencies, this makes sense from a wave observation standpoint. The long growth time compared to the scattering time justifies the quasistationary assumption. Since He⁺ and H⁺ wave growth rates must be computed independently, wave excitation by one species of PUI has no effect on the wave spectra that are used when computing the other. Since our theory is based on the assumption that pickup He⁺ is scattered, and stays in an asymptotic form as more particles are ionized and contribute to wave growth, we want the scattering time to be short compared to the wave growth time.

5 Turbulence Rates

Although we are searching for waves, and not turbulence, it is important to understand how turbulence works. In interplanetary space, the solar wind and the magnetic field fluctuations act like a turbulent MHD flow. Waves are being constantly generated, but the turbulence can easily overwhelm these low-frequency waves and dissipate the energy. This process is called the turbulent cascade. It moves the fluctuation energy from large scales, like transient

flow, to the smallest scales of kinetic dissipation. It has been found that the temperature of solar wind protons as they flow away from the sun is higher than it should be, when considering adiabatic cooling from the expansion of the solar wind. The turbulent cascade is ultimately responsible for the energy that heats this background plasma. Simple turbulent scaling laws show that the measured spectrum of fluctuations agrees with the rate of thermal proton heating. Turbulent transport theory can successfully reproduce the fluctuation power, correlation length, cross helicity, and proton heating from 0.3 to 100 AU at both high and low latitudes [Zhou & Matthaeus(1990a), Zhou & Matthaeus(1990b), Matthaeus et al.(1994), Zank et al.(1996), Smith et al.(2001), Smith et al.(2006a), Isenberg, Smith & Matthaeus(2003), Isenberg(2005), Isenberg et al.(2010), Breech et al.(2005), Breech et al.(2008), Breech et al.(2009), Breech et al.(2010), Usmanov & Goldstein(2006), Usmanov et al.(2011), Usmanov et al.(2012), Usmanov et al.(2014), Usmanov et al.(2016), Usmanov et al.(2018), Ng et al.(2010), Oughton et al.(2011), Zank(2012), Adhikari et al.(2015a), Adhikari et al.(2015b), Adhikari et al.(2017), Zank et al.(2017)].

The general method for measuring the rate of energy cascade through the turbulent inertial range comes from third-moment theory. [Politano & Pouquet(1998a), Politano & Pouquet(1998b), MacBride et al.(2008), Stawarz et al.(2009), Stawarz et al.(2010), Stawarz et al.(2011), Coburn et al.(2012), Coburn et al.(2014), Coburn et al.(2015), Smith(2009), Smith et al.(2018)] This method agrees with the rate of thermal proton heating [Vasquez et al.(2007)]. There are multiple theories for turbulent dynamics, that vary the time scales for things like energy transport through the spectrum and the characteristic lifetimes of individual fluctuations. The theory we use is the most traditional view. It is an extension of Kolmogorov's hydrodynamic theory [Kolmogorov(1941a)], adapted for MHD [Matthaeus & Zhou(1989), Leamon et al.(1999), Smith(2009), Matthaeus & Velli(2011)]. It uses the amplitude of the power spectrum to predict the energy transport rate through the spatial scales of the inertial range. We rescale the overall amplitude of the cascade rate in order to match the observed proton heating rate [Vasquez et al.(2007), Montagud-Camps, Grappin & Verdini(2018)]. This gives us

$$\epsilon = \frac{f^{5/2}[E(f)]^{3/2} \cdot 21.8^3}{V_{SW} N_P^{3/2}} \quad (4)$$

where $E(f)$ is the measured magnetic field power spectral density in units of $\text{nT}^2 \text{Hz}^{-1}$. It is assumed to vary as $f^{-5/3}$. N_P and 21.8^3 are part of the conversion of the magnetic field to Alfvén units, and ϵ is given in units of $\text{km}^2 \text{s}^{-3}$. We assume equipartition of kinetic and magnetic energy so that the Alfvén ratio $R_A = 1$ [Vasquez et al.(2007)]. This theory is the likely explanation for the dominant two-dimensional fluctuations seen in wave vectors that are quasi-perpendicular to the mean magnetic field.

In the equation above we assume a consistent $f^{-5/3}$ prediction for the background power spectra. This does not always agree with the power spectra we study, which vary significantly in intensity. This could be because the data intervals we analyze are relatively

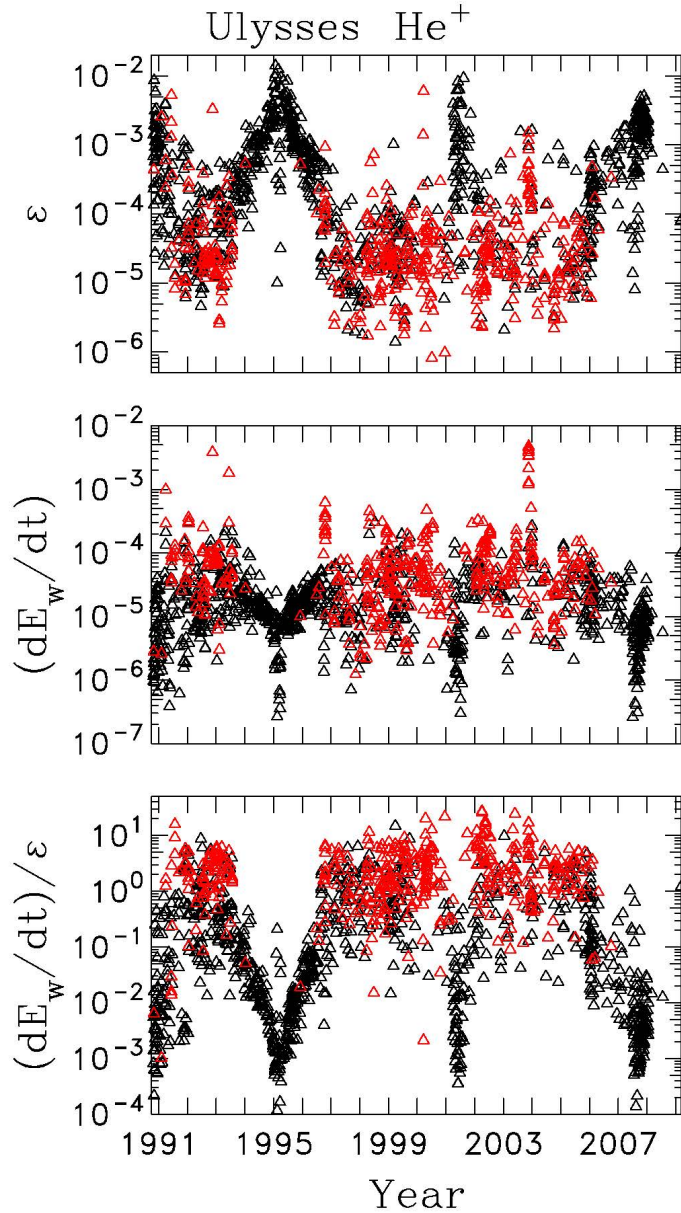


Figure 7: (top) Turbulent energy transport rate epsilon in units of $\text{km}^2 \text{s}^{-3}$ evaluated using the background spectrum (minus any enhanced wave power due to suprathermal ions) evaluated at $f_{\text{He},c}$. (middle) Wave excitation rate (dE_W/dt) for newborn interstellar pickup He⁺ in units of $\text{km}^2 \text{s}^{-3}$. (bottom) Ratio of rates showing that wave growth is favored outside the fast latitude scans, so when the spacecraft is at lower latitudes and greater heliocentric distances. This plot reproduced from Marchuk et al. (2021).

short. The wave events in the data are often only visible for a brief duration, and the data intervals are short to properly capture them. It is known that short samples of data do not regularly agree with averages of large volumes of data. We also know that measurement noise flattens spectra when the overall spectral amplitude is reduced sufficiently - this can be observed in the Voyager data. We believe that this scaling of the cascade is still a reasonable place to begin applying turbulence ideas.

Figure 7 visualizes these concepts well. The top panel shows the average rates we calculated to show energy moving through the inertial range of turbulence. The slower the turbulence rate is, the more likely the wave energy is to accumulate. It depends strongly on heliocentric distance. We know this because wave events most often appear in more distant measurements, better seen in Figure 12. They are absent from fast latitude scans at solar minimum (turbulence rates are higher), but are common during those of the solar maximum. This appears to be not due to the physics of PUI scattering and waves but directly caused by variations in turbulence connected to the solar cycle.

The middle panel shows H^+ wave growth rates over the same intervals. It look different mainly because the primary mode of He^+ ionization is solar EUV photons, and neutral He density is dependent on heliocentric distance to the point where it can compensate for the distribution of solar EUV photons. We can see that wave growth rates are higher for wave events than the background intervals. The bottom panel shows the ratio of wave growth to turbulence rates. It shows nicely that wave events occur when the growth rate is close to, or exceeds, the turbulence rate. From this we conclude that waves are always being generated, but are only observed at growth rates strong enough to overcome the turbulence.

Figure 8 shows the same concept as the last panel of Figure 7, but with all controls and events graphed with the ratio of wave growth rate to turbulence rate over the ellipticity. We can see that wave events occur when the growth rate is comparable or greater than the turbulence rate. It also demonstrates an earlier statement, that low ellipticity in an interval indicates no wave activity, which is clear from the line of controls along 0 ellipticity.

6 Data Analysis

Several different spectral analysis techniques were used to identify wave and control intervals in this study. The first step was to download the entirety of the one second magnetic field observations from the Ulysses FGM instrument [Balogh et al.(1992), Bame et al.(1992)]. Using Fast Fourier Transform (FFT) techniques [Fowler, Kotich & Elliott(1967), Rankin & Kurtz(1970), Means(1972), Mish et al.(1982), Argall et al.(2015), Argall et al.(2017), Fisher et al.(2016), Hollick et al.(2018a)], this data was used to produce automated daily spectrograms. We identified these candidate intervals by looking at the spectrograms for large patches of color in the ellipticity panel. Other panels do not show the wave event as clearly - the power spectrum covers an extended range of values and any enhancement is comparatively too small to easily see. Sometimes in spectrograms, the cadence of the

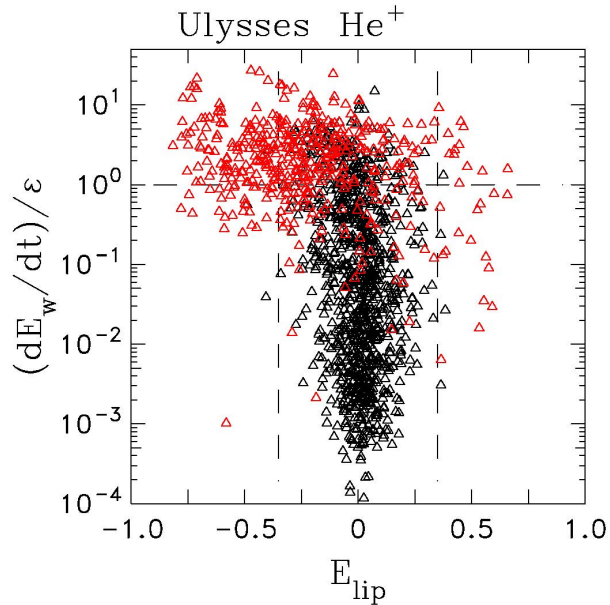


Figure 8: The ratio of the wave growth rate to the turbulence rate $(dE_w/dt)/\epsilon$ showing that waves, as represented by times of high $E_{lip} < -0.25$, are seen during times of favorable growth rates. This plot reproduced from Marchuk et al. (2021).

magnetic field data changes within the two days, which changes the Nyquist frequency. This is normal for Ulysses data. Any gaps that occur originate from the changing measurement cadence - the change renders the spectrum uncomputed.

Once we select likely wave intervals, we analyze their power spectra. The power spectrum is produced by putting the data from the time intervals through a combination of a prewhitened Blackman-Tukey analysis and an FFT analysis. At the same time, we create a polarization analysis by Fourier transforming the time series. The time series plots are made from one minute FGM data that is downloaded and compiled into 10 day plots for reference - these are useful for identifying potential discontinuities like shocks.

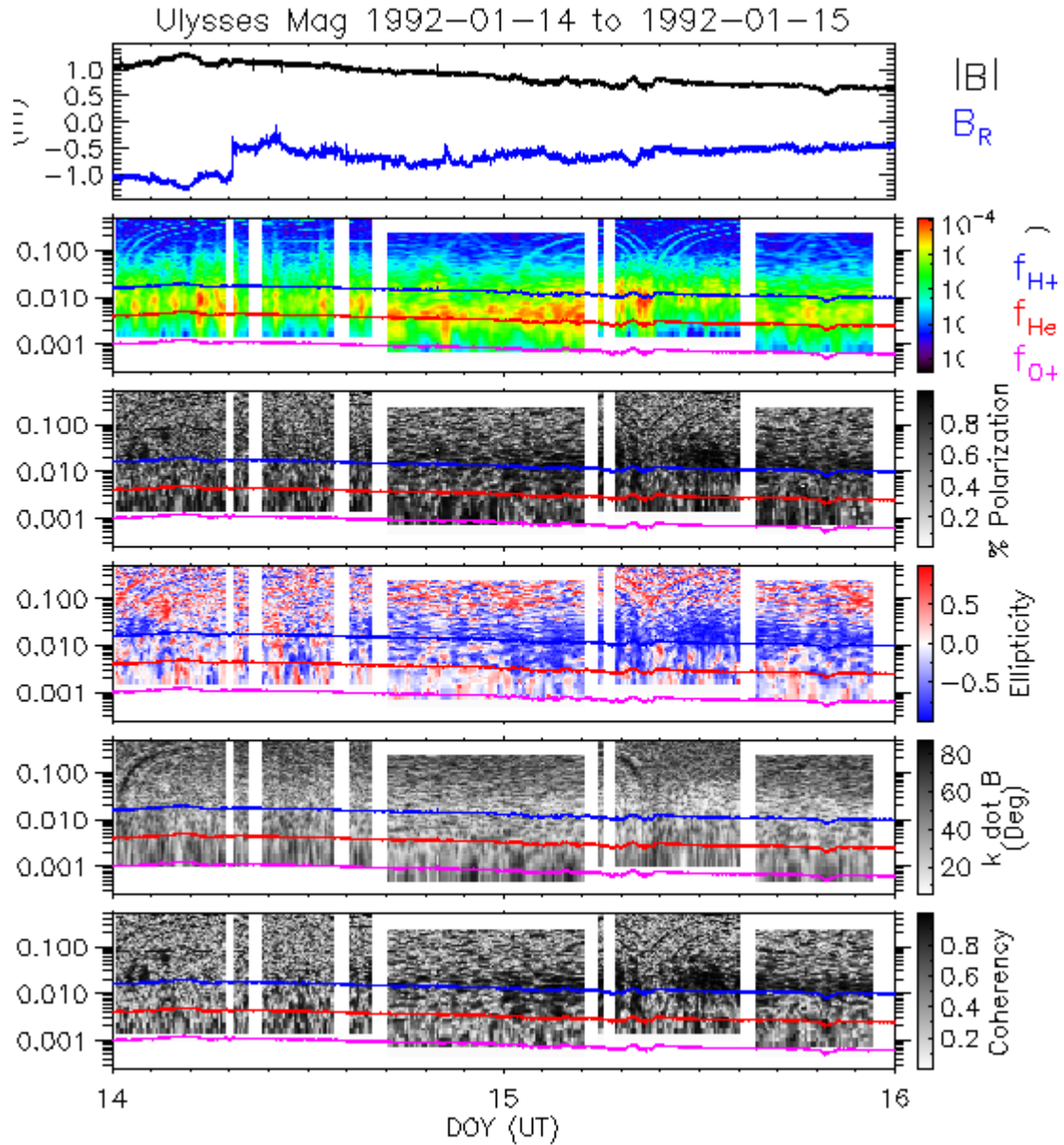


Figure 9: Example of the daily spectrograms used to locate the wave events studied here. The data analyzed are DOYs 14–15 of 1992. The spectrogram shows (top to bottom) the time series for B and B_R in heliocentric (R, T, N) coordinates. The second panel shows the power spectrum followed by the degree of polarization. Next is the ellipticity and then the angle between the minimum variance direction and the mean magnetic field. The last panel is the coherence. Horizontal lines represent the cyclotron frequency of H^+ , He^+ , and O^+ . This plot reproduced from Marchuk et al. (2021).

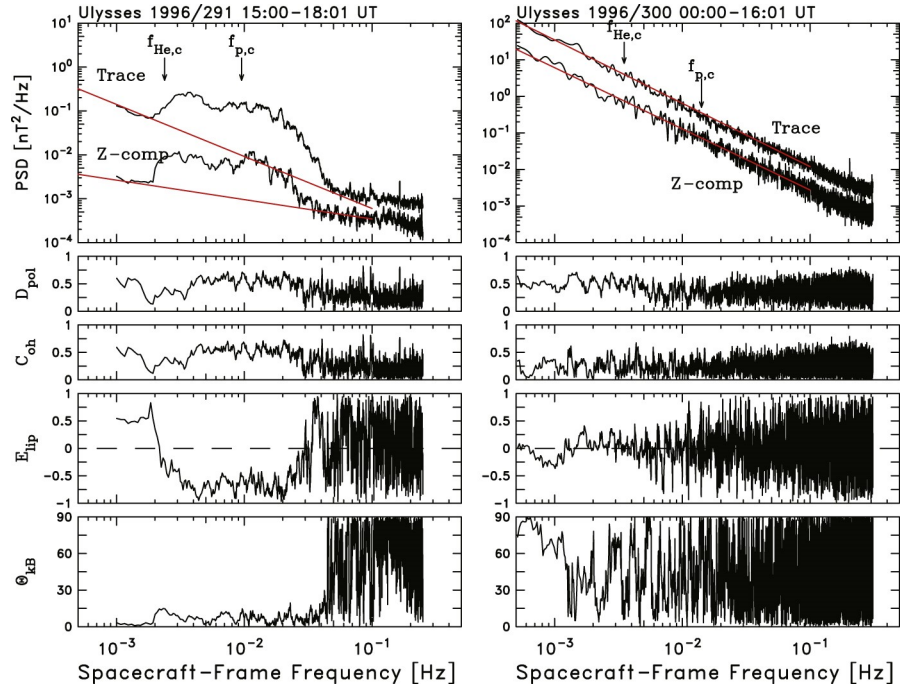


Figure 10: Examples of spectra used in this study. (left) Wave interval arising from pickup He+ on DOY 291 of 1996. (right) Control interval dominated by turbulence dynamics on DOY 300 of 1996. This plot reproduced from Marchuk et al. (2021). More analysis in section 7.

7 Ulysses Observations

Our observations come from one-second magnetic field observations from the Flux Gate Magnetometer (FGM) on the Ulysses spacecraft [Bame et al.(1992), Balogh et al.(1992)]. The spacecraft launched in late 1990, and it was operational until June of 2009. Our first observation is on day 299 of 1990, and our last is on day 70 of 2009. Thermal ion measurements, which we also use, are from the Solar Wind Observations over the Poles of the Sun (SWOOPS) instrument, which provides solar wind speed and density data. Our final event list had 1479 data intervals showing waves due to He^+ and H^+ and ambient turbulence. This was split into one set with 452 intervals of He^+ waves and 962 control intervals, which may have H^+ waves but should not contain He^+ waves. In these figures, any red triangles are He^+ wave events, and black squares are control intervals.

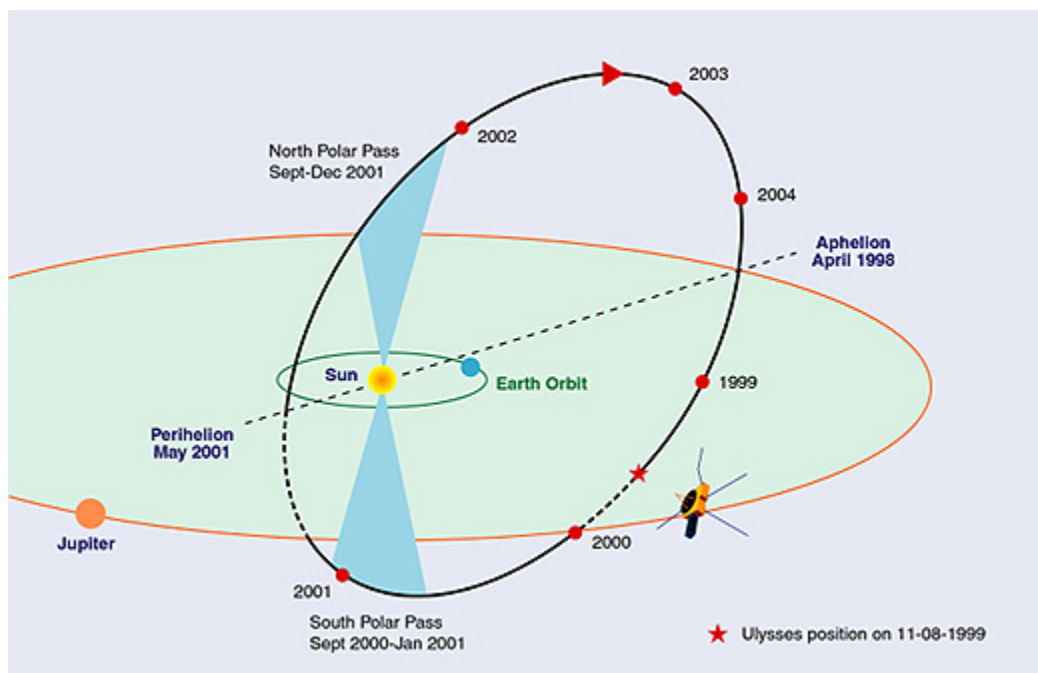


Figure 11: Ulysses' second orbit (1999–2004) Image Credit: NASA (public domain)

The trajectory of the Ulysses spacecraft, shown in Figures 11 and 12, began with a straight line to Jupiter, where it performed a gravity assist to launch itself out of the plane of the ecliptic and towards the Sun. It transited over the southern and northern poles of the Sun three times performing fast latitude scans before it froze. Figure 12 shows the heliocentric distance of Ulysses in AU and the latitude in degrees in the first panel, and the second panel shows heliolongitude. The third panel shows the time and duration of every interval we studied. Most events are at a moderate to low heliolatitude beyond 3AU. This

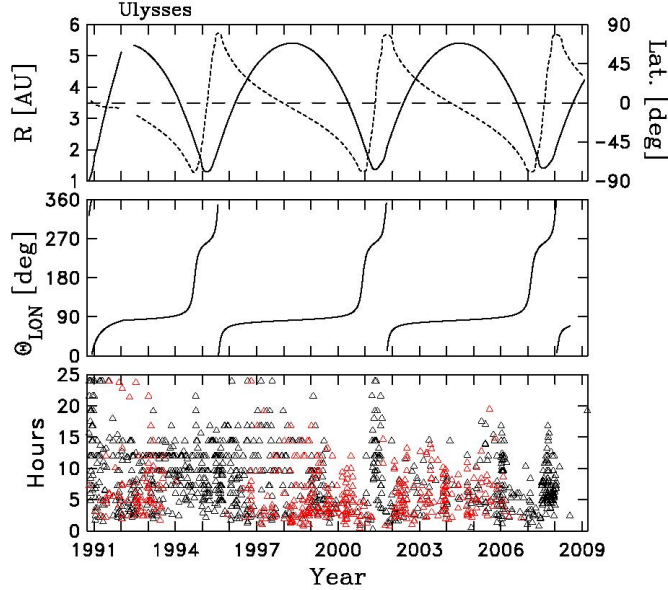


Figure 12: Trajectory of the Ulysses spacecraft. (top) Heliocentric distance R (solid curve) and heliolatitude (dashed curve) of the spacecraft as a function of time. (second panel) Heliolongitude that mostly reflects the Sun’s rotation as the spacecraft orbits on a fixed plane. (third panel) Time and duration of the data intervals studied here. Red triangles represent times when wave signatures are seen at frequencies normally associated with newborn interstellar pickup He^+ . Black squares represent control intervals when wave signatures are not seen in the frequency range $f_{\text{He},c} \leq f_{sc} \leq f_{p,c}$. Control intervals may contain waves due to pickup H^+ . This plot reproduced from Marchuk et al. (2021)

might reflect either the nature of the orbit, since the spacecraft spent more time beyond 3AU, or it might be due to turbulence conditions. We do however find waves due to helium at high latitudes inside 3.5AU. H^+ does not get inside 3AU, so wave excitation by this species is not observed there. Fast latitude scans usually have no wave observations.

Wave events can be categorized into H^+ and He^+ events by frequency. When enhancements occur in the ellipticity in the range $f_{\text{He},c} < f_{sc} < f_{p,c}$ we conclude that these waves are likely due to pickup He^+ . Higher frequency waves that are above the proton cyclotron frequency are generally pickup H^+ , although they could also be scattered He^+ . This is most easily seen in the large blue or red patches in the ellipticity panels of spectrograms.

In the spectrogram in Figure 9, showing data from day 291 - 292 of 1996, the large blue area is a great example. He^+ and H^+ examples can be seen here. It is possible that there are waves due to either pickup H^+ or scattered He^+ , but it is unclear without further analysis. One way to analyze that would be to compare the wave growth rate of newborn interstellar

pickup H^+ to the turbulence rate to see if it is a good candidate for wave growth. In these spectrograms, the first panel is the time series for B and B_R in heliocentric (R,T,N) coordinates. In this panel R is directed from the Sun to the point of the measurement, T is coplanar with the Sun's rotational equator and directed in the sense of rotations, and $N = R \times T$. Below this is the power spectrum and then the degree of polarization. Next is ellipticity, carrying the sign of the polarization, and then the angle between the minimum variance direction and the mean magnetic field from the subinterval used to compute the spectrum. The last panel is coherence. The horizontal lines on five panels are the cyclotron frequencies of H^+ , He^+ and O^+ (top to bottom).

Analyzing the polarization and power spectrum is important to confirm a wave event. In Figure 10, we see significant results to confirm a wave event - the wave event is on the left and the right is a control event. The top panels of the power spectra plots are the trace of the power spectral matrix and the spectrum of the field-aligned fluctuations (Z -comp). There are fit lines for these spectra in red to demonstrate the background spectra without the wave-generated enhancement. Examining these spectra can assist in identification of waves because it is easier to see the frequency at which a wave occurs, and whether it is in the range for He^+ , H^+ , or both. Below these panels are spectra for degree of polarization, coherence, ellipticity, and the angle between the minimum variance direction and the mean magnetic field.

A wave enhancement visible in the first panel should be visible in all the panels below it. In the left column, there is a large power enhancement at frequencies above the helium cyclotron frequency, which indicates excited pickup He^+ . It exceeds the power in the parallel component by a factor of about 10, which is expected from theory and means the fluctuations are transverse to the mean magnetic field and therefore noncompressive [Lee & Ip(1987)]. The ellipticity in this range is about -1, which is also expected, and this indicates that the fluctuations are left-hand polarized in the spacecraft frame. If the waves are sunward propagating as theory predicts, then these waves should be right-hand polarized in the plasma frame. It is possible that this interval also shows evidence of H^+ wave activity.

The right side of Figure 10 is a control interval. This is from a stream interaction region, or a place where the fast solar wind and slow solar wind meet. These are generally regions of enhanced turbulence levels. There is no evidence of any waves from PUIs, and no enhancement anywhere in the spectrum. There were several shock candidates in the general vicinity of the interval, but we have not analyzed them since there is no evidence of waves from any source during this time. Comparing this to the left side of the figure shows clearly how much a wave event can alter the analysis.

8 Ongoing Research

Our search for low-frequency He^+ waves excited by newborn interstellar pickup ions, revealed He^+ and H^+ events over the full range of heliodistances and heliolatitudes in the Ulysses orbit, except for H^+ events within 3 AU. We also see pickup ion waves in Voyager data [Joyce et al.(2010), Aggarwal et al.(2016), Hollick et al.(2018a), Hollick et al.(2018b), Hollick et al.(2018c), Joyce et al.(2012)]. However, in our search of Ulysses data we found several high-frequency wave events. These events are quite unlikely to have the same pickup ion source, because the polarization changes sign without regard to the mean magnetic field. This work is ongoing, and as such we are considering several different options for their possible source. One theory is that the waves are due to anisotropies in the thermal proton distribution. This could excite waves propagating in both directions, with one wave appearing to have the wrong polarization due to the Doppler shift into the spacecraft frame. We hope to find a high frequency wave event without a concurrent low frequency wave, which would greatly assist the interpretation. We do not have one now because the database was built on low-frequency wave events. Figure 13 is an example of the power spectra for three wave events we believe to be good candidates for these high-frequency waves.

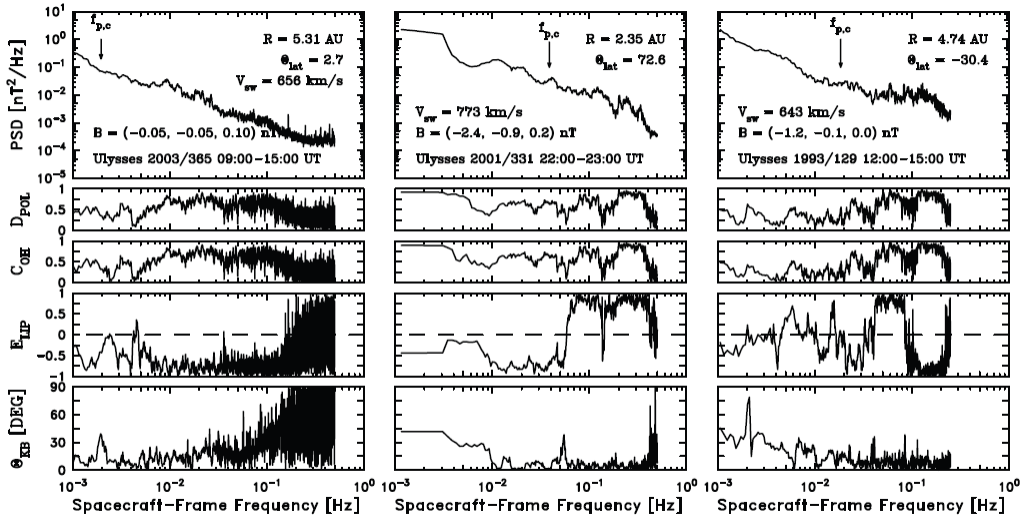


Figure 13: An example of the power spectra for three wave events that we believe to be high-frequency wave events excited by thermal anisotropy.

9 Summary

We have shown evidence of waves excited by newborn interstellar pickup ions. Interstellar neutrals pass through the heliosphere, and are ionized by various processes such as collision with a charged solar wind particle (H^+), or by an extreme ultraviolet solar photon (He^+). As neutrals they are effectively stationary compared to the solar wind speed, but are picked up once ionized and flow at the solar wind speed. The Lorentz force causes the PUIs to orbit the field at the ion cyclotron frequency. When the particles resonate with other MHD waves, they scatter, and this cyclotron resonant instability generates waves.

Distribution of neutrals and pickup ions varies across the solar system. Gloeckler et al.(2004) describes a gravitational focusing cone of helium behind the Sun, and Zank (2016) discusses relative hydrogen distribution in the heliosphere. H^+ PUIs cannot penetrate within 3 AU of the Sun, but He^+ can.

Wave events were selected first by inspecting daily spectrograms for evidence of high ellipticity. These intervals are reanalyzed using a library of preexisting spectral codes to look for wave enhancements in the power spectrum for each event. The final event list contains 1479 data intervals, of which 452 show evidence of He^+ waves and 962 are controls. Some controls have waves due to H^+ , but they have no waves in the He^+ frequency range.

Wave observation depends on turbulence rates. While waves are constantly being generated, turbulence can easily overwhelm the wave energy. The energy dissipated by turbulence is transported to small scales, and eventually heats the background plasma. Beyond 10 AU, these waves provide the dominant energy source to drive turbulence and heat background plasma. When the turbulence is low enough that wave energy can accumulate to sufficient levels, the wave energy is observable and can be measured. By comparing the wave growth rate to the turbulence rate, we see that waves are visible when the growth rate is close to or higher than the turbulence rate. A high ellipticity is also indicative of a wave event. Near zero ellipticity indicates no wave activity. We see most events at moderate to low heliolatitude beyond 3 AU, either due to the nature of the orbit or turbulence conditions, although He^+ events do occur within 3.5 AU at high latitudes.

10 Russian Translation

As part of my Russian major capstone, I translated a summary of my thesis into Russian in an academic writing style with the assistance of my professor, Dr. Ekaterina Burvikova.

Абстракт

Были использованы наблюдения магнитного поля из магнитометра на спутнике Улисс чтобы найти примеры низкочастотных магнитных волн в результате рассеивания ионов гелия, которые называются pickup ions (PUIs). Считается, что всегда есть волны, но они только видны, когда скорость роста волновой энергии больше, чем турбулентность. Гелиевые волны были измерены по всей орбите Улисса.

Учёные хотят лучше понимать, как работает солнечная система. Одной из актуальных проблем в этой части космической физики является понимание низкочастотных магнитных волн. Нейтральные атомы гелия, прилетающие в Солнечную систему из межзвёздного космоса, становятся ионизированными. Они называются pickup ions (PUIs). Для понимания этих ионов важно изучение солнечного ветра.

Нет одного места, где заканчивается атмосфера Солнца. Солнечный ветер дует с Солнца. Ветер состоит из заряженных частиц. Большинство из этих частиц - протоны и электроны. Медленный солнечный ветер имеет скорость 250–400 км/с и быстрый солнечный ветер имеет скорость 400–800 км/с. Солнечный ветер связан с магнитным полем Солнца.

Солнечная система находится в центре гелиосферы. Гелиосфера - часть космоса, на которую влияют магнитное поле Солнца и солнечный ветер. Защищая магнитное поле Солнца не допускает большинство заряженных частиц в гелиосферу. Большие облака нейтрального газа в межзвёздном космосе могут войти в гелиосферу, потому что нейтральный газ не вступает во взаимодействие с магнитным полем Солнца. Эти нейтральные атомы, расположенные в гелиосфере, ионизируются. Для атомов водорода ионизация появляется из-за отдачи электрона нейтральным атомом. Для гелия ионизация возникает из-за передачи атома экстремальным ультрафиолетовым фотоном. Ионы вращаются вокруг линии магнитного поля. Когда ионы гелия рассеиваются, этот процесс создаёт низкочастотные магнитные волны. Волны только видно, когда скорость роста волновой энергии больше, чем турбулентность. Волновая энергия всегда существует, но создание волн занимает много времени. Высокий уровень турбулентности разрушает волновую энергию и волны. Ионы быстро рассеиваются, но время роста волн продолжительное.

Солнечный ветер и магнитное поле действуют как турбулентный поток. Ионы всегда создают волны, но турбулентность всегда их разрушает. Было измерено, что солнечный ветер далеко от Солнца горячее, чем должен быть. Теория турбулентного переноса утверждает, что разрушение волн нагревает ветер далеко от Солнца.

Данные, полученные при помощи магнитометра на спутнике Улисс, предназначены для анализа волн ионов гелия. Из данных были сделаны фотографии как 9. Рассмотр-

им на примере. На фотографии видны красные или синие очертания, которые означают что есть волна. Нами было выбрано время, и составлен список из времени волн. Список был послан в программу, которая создаёт графики. На графике как 10 видно, были ли очертания волнами или не были. Частота волны была рассмотрена, чтобы узнать. Налево в графике есть пример волны, и направо нет. Тогда можно составить официальный список событий. Были использованы наблюдения магнитного поля из магнитометра на спутнике Улисс. Улисс был запущен в 1990 году, и замёрз в 2009 году. Финальный список состоит из 1479 временных интервалов. Были 452 с волнами ионов гелия, и 962 с турбулентностью или с волнами ионов водорода. На рисунке 14, видна карта траектории спутника. У спутника была необычная траектория. Спутники обычно летают в плоскости эклиптики, а Улисс — нет. Вовремя исследования, гелиевые волны были измерены по всей орбите Улисса. Некоторые из этих волн имеют высокие частоты. Ещё неизвестно, что создало эти волны. Примеры видны на графике 13. Одна теория утверждает, что эти высокочастотные магнитные волны создаются анизотропией в тепловом распределении протонов. Теория будет улучшена, когда в процессе исследования найдётся больше волн.

Основные результаты исследования заключаются в следующем: что волны всегда существуют, но видимость волн зависит от турбулентности; что далеко от Солнца, разрушение волн меняет температуру солнечного ветра; и что ещё неизвестно, почему некоторые волны имеют высокие частоты.

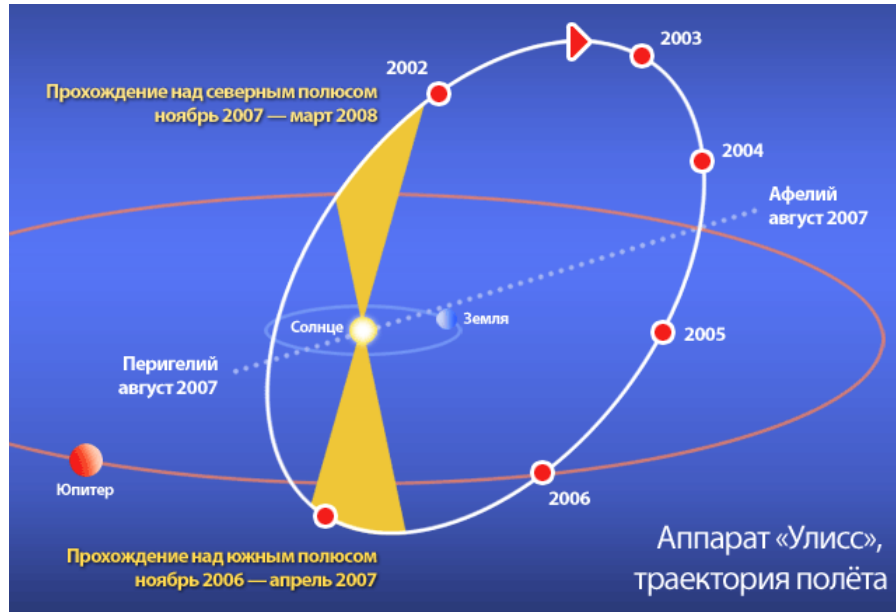


Figure 14: Траектория полёта Улисса. Image is in the public domain.

Acknowledgements

I have a lot of people that I'd like to thank in the final work of my UNH career. First, my advisor Dr. Charles Smith. Thank you for hiring a high schooler to examine PNG files for you. Oh, and the several years' worth of advice, lunches, and space plasma physics explanations, too. You've inspired me to give it a go in the physics world.

Thank you to my professors here at UNH, particularly Profs. Hollen, Meredith, and Burvikova. The three of you are exceptionally good teachers who made attending this school worth it. And sorry I kept turning in my homework late. Катя, спасибо огромное за все!

Thank you to my family and friends for all your support! I sure do complain a lot, but I promise that I do actually like physics. Thanks for listening anyway. And reminding me that I do actually understand it, even when I think I don't. In the interest of brevity you will all have to know who you are - my family and partner, old and new friends, physicists and fencers, and every advisor I've adopted along the way. If you've read this far you certainly fit into some of these - feel free to contact me to find out which one. It takes a village to graduate a double major.

And finally, a special apology to anyone I've ever put through explanations of my research work, which have been known to have varying levels of quality (although I hope they've improved, over the years). With any luck, this document may clear up some of your questions.

References

- Adhikari, L., Zank, G. P., Bruno, R., Telloni, D., Hunana, P., Dosch, A., Marino, R., & Hu, Q. 2015a, ApJ, 805, 63
- Adhikari, L., Zank, G. P., Bruno, R., Telloni, D., Hunana, P., Dosch, A., Marino, R., & Hu, Q. 2015b, J. Physics: Conf. Series, 642, 012001
- Adhikari, L., Zank, G. P., Hunana, P., Shiota, D., Bruno, R., Hu, Q., & Telloni, D. 2017, ApJ, 841, 85
- Aggarwal, P., Taylor, D. K., Smith, C. W., Joyce, C. J., Fisher, M. K., Isenberg, P. A., Vasquez, B. J., Schwadron, N. A., Cannon, B. E., & Richardson, J. D. 2016, ApJ, 822, 94
- Argall, M. R., Fisher, M. F., Joyce, C. J., Smith, C. W., Isenberg, P. A., Vasquez, B. J., Schwadron, N. A., & Skoug, R. M. 2015, Geophys. Res. Lett., 42, 9617-9623
- Argall, M. R., Hollick, S. J., Pine, Z. B., Smith, C. W., Joyce, C. J., Isenberg, P. A., Vasquez, B. J., Schwadron, N. A., Sokół J. M., Bzowski, M., Ness, N. F., & Burlaga, L. F. 2017, ApJ, 849, 61

- Balogh et al., *Astron. Astrophys. Suppl. Ser.* 92, 221-236, 1992.
- Bame, S. J., McComas, D. J., Barraclough, B. L., Phillips, J. L., Sofaly, K. J., Chavez, J. C., Goldstein, B. E., & Sakurai, R. K.: 1992, 'The Ulysses Solar Wind Plasma Experiment', *Astron. Astrophys. Suppl. Ser.* 92, 237.
- Breech, B., Matthaeus, W. H., Minnie, J., Oughton, S., Parhi, S., Bieber, J. W., & Bavasano, B. 2005, *Geophys. Res. Lett.*, 32, L06103
- Breech, B., Matthaeus, W. H., Minnie, J., Bieber, J. W., Oughton, S., Smith, C. W., & Isenberg, P. A. 2008, *J. Geophys. Res.*, 113, A08105
- Breech, B., Matthaeus, W. H., Cranmer, S. R., Kasper, J. C., & Oughton, S. 2009, *J. Geophys. Res.*, 114, A09103
- Breech, B., Cranmer, S. R., Matthaeus, W. H., Kasper, J. C., & Oughton, S. 2010, Twelfth International Solar Wind Conference, 214-217
- Cannon, B. E., Smith, C. W., Isenberg, P. A., Vasquez, B. J., Joyce, C. J., Murphy, N., & Nuno, R. G. 2013, *Solar Wind 13, AIP Conf. Proc.* 1539, 334-337
- Cannon, B. E., Smith, C. W., Isenberg, P. A., Vasquez, B. J., Murphy, N., & Nuno, R. G. 2014a, *ApJ*, 784, 150
- Cannon, B. E., Smith, C. W., Isenberg, P. A., Vasquez, B. J., Joyce, C. J., Murphy, N., & Nuno, R. G. 2014b, *ApJ*, 787, 133
- Cannon, B. E., Smith, C. W., Isenberg, P. A., Vasquez, B. J., Joyce, C. J., Murphy, N., & Nuno, R. G. 2017, *ApJ*, 840, 13
- Coburn, J. T., Smith, C. W., Vasquez, B. J., Stawarz, J. E., & Forman, M. A. 2012, *ApJ*, 754, 93
- Coburn, J. T., Smith, C. W., Vasquez, B. J., Forman, M. A., & Stawarz, J. E. 2014, *ApJ*, 786, 52
- Coburn, J. T., Forman, M. A., Smith, C. W., Vasquez, B. J., & Stawarz, J. E. 2015, *RSPTA*, 373, 20140150
- Fisher, M. K., Argall, M. R., Joyce, C. J., Smith, C. W., Isenberg, P. A., Vasquez, B. J., Schwadron, N. A., Skoug, R. M., Sokół J. M., Bzowski, M., Zurbuchen, T. H., & Gilbert, J. A. 2016, *ApJ*, 830, 47
- Fowler, R. A., Kotick, B. J., & Elliott, R. D. 1967, *J. Geophys. Res.*, 72(11), 28712883

- Gloeckler, G., Möbius, E., Geiss, J., Bzowski, M., Chalov, S. V., Fahr, H. J., McMullin, D. R., Noda, H., Oka, M., Rucinski, D. K., Skoug, R. M., Terasawa, T., Steiger, R. V., Yamazaki, A., & Zurbuchen, T. H., 2004, *A&A*, 426, 845-854.
- Hollick, S. J., Smith, C. W., Pine, Z. B., Argall, M. R., Joyce, C. J., Isenberg, P. A., Vasquez, B. J., Schwadron, N. A., Sokół, J. M., Bzowski, M., & Kubiak, M. A. 2018a, *ApJ*, 863, 75
- Hollick, S. J., Smith, C. W., Pine, Z. B., Argall, M. R., Joyce, C. J., Isenberg, P. A., Vasquez, B. J., Schwadron, N. A., Sokół, J. M., Bzowski, M., & Kubiak, M. A. 2018b, *ApJ*, 863, 76
- Hollick, S. J., Smith, C. W., Pine, Z. B., Argall, M. R., Joyce, C. J., Isenberg, P. A., Vasquez, B. J., Schwadron, N. A., Sokół, J. M., Bzowski, M., & Kubiak, M. A. 2018c, *ApJS*, 237, 34
- Isenberg, P. A., Smith, C. W., & Matthaeus, W. H. 2003, *ApJ*, 592, 564-573
- Isenberg, P. A. 2005, *ApJ*, 623, 502-510
- Isenberg, P. A., Smith, C. W., Matthaeus, W. H., & Richardson, J. D. 2010, *ApJ*, 719, 716-721
- Joyce, C. J., Smith, C. W., Isenberg, P. A., Murphy, N., & Schwadron, N. A. 2010, *ApJ*, 724, 1256-1261
- Joyce, C. *Electromagnetic Waves Excited by Newborn Interstellar Pickup Ions: Examination of Voyager Observations from 1 to 4.5AU*, 2011, University of New Hampshire
- Joyce, C. J., Smith, C. W., Isenberg, P. A., Gary, S. P., Murphy, N., Gray, P. C., & Burlaga, L. F. 2012, *ApJ*, 745, 112
- Kallenrode, May-Britt. (2004). *Space physics: an introduction to plasmas and particles in the heliosphere and magnetospheres*. Advanced texts in physics. Berlin: Springer, 2004.
- Kolmogorov, A. N. 1941a, *Dokl. Akad. Nauk SSSR*, 30, 301-305. (Reprinted in *Proc. R. Soc. London A*, 434, 9-13, 1991.)
- Leamon, R. J., Smith, C. W., Ness, N. F., & Wong, H. K. 1999, *J. Geophys. Res.*, 104, 22,331-22,344
- Lee, M. A., & Ip, W.-H. 1987, *J. Geophys. Res.*, 92, 11,041-11,052
- MacBride, B. T., Smith, C. W., & Forman, M. A. 2008, *ApJ*, 679, 1644
- Marchuk, A. V., Smith, C. W., Watson, A. S., et al. 2021, *ApJ*, 923, 185

- Matthaeus, W. H., & Zhou, Y. 1989, *Phys. Fluids B*, 1(9), 1929-1931
- Matthaeus, W. H., & Velli, M. 2011, *Space Sci. Rev.*, 160, 145-168
- Matthaeus, W. H., Oughton, S., Pontius, Jr., D. H., & Zhou, Y. 1994, *J. Geophys. Res.*, 99, 19,267-19,287
- Means, J. D. 1972, *J. Geophys. Res.*, 77(28), 55515559
- Mish, W. H., Wenger, R. M., Behannon, K. W., & Byrnes, J. B. 1982, *Interactive Digital Signal Processor, NASA Technical Memorandum 83997*, Goddard Space Flight Center, Greenbelt, MD. (Revised 1984.)
- Montagud-Camps, V., Grappin, R., & Verdini, A. 2018, *ApJ*, 853, 153
- Murphy, N., Smith, E. J., Tsurutani, B. T., Balogh, A., & Southwood, D. J. 1995, *Space Sci. Rev.*, 72(1-2), 447-453
- Ng, C. S., Bhattacharjee, A., Munsi, D., Isenberg, P. A., & Smith, C. W. 2010, *J. Geophys. Res.*, 115, A02101
- Oughton, S., Matthaeus, W. H., Smith, C. W., Breech, B., & Isenberg, P. A. 2011, *J. Geophys. Res.*, 116, A08105
- Pine, Z. B., Smith, C. W., Hollick, S. J., Argall, M. R., Vasquez, B. J., Isenberg, P. A., Schwadron, N. A., Joyce, C. J., Sokół, J. M., Bzowski, M., Kubiak, M. A., & McLaurin, M. L. 2020, *ApJ*, 900, 94
- Politano, H., & Pouquet, A. 1998a, *Phys. Rev. E*, 57(1), R21
- Politano, H., & Pouquet, A. 1998b, *Geophys. Res. Lett.*, 25, 273
- Rankin, D., & Kurtz, R. 1970, *J. Geophys. Res.*, 75(28), 54445458.
- Smith, C. W. 2009, Chapter 7 in *Heliophysics I. Plasma Physics of the Local Cosmos*, edited by C. J. Schrijver and G. Siscoe, Cambridge University Press
- Smith, C. W., Matthaeus, W. H., Zank, G. P., Ness, N. F., Oughton, S., & Richardson, J. D. 2001, *J. Geophys. Res.*, 106, 8253-8272
- Smith, C. W., Isenberg, P. A., Matthaeus, W. H., & Richardson, J. D. 2006a, *ApJ*, 638, 508-517
- Smith, C. W., Vasquez, B. J., Coburn, J. T., Forman, M. A., & Stawarz, J. E. 2018, *ApJ*, 858, 21

- Sokół, J. M., McComas, D. J., Bzowski, M., & Tokumaru, M. 2020, *ApJ*, 897, 179, 10.3847/1538-4357/ab99a4
- Stawarz, J. E., Smith, C. W., Vasquez, B. J., Forman, M. A., & MacBride, B. T. 2009, *ApJ*, 697, 1119-1127
- Stawarz, J. E., Smith, C. W., Vasquez, B. J., Forman, M. A., & MacBride, B. T. 2010, *ApJ*, 713, 920
- Stawarz, J. E., Vasquez, B. J., Smith, C. W., Forman, M. A., & Klewicki, J. C. 2011, *ApJ*, 736, 44
- Usmanov, A. V., & Goldstein, M. L. 2006, *J. Geophys. Res.*, 111, A07101
- Usmanov, A. V., Matthaeus, W. H., Breech, B. A., & Goldstein, M. L. 2011, *ApJ*, 727, 84
- Usmanov, A. V., Goldstein, M. L., & Matthaeus, W. H. 2012, *ApJ*, 754, 40
- Usmanov, A. V., Goldstein, M. L., & Matthaeus, W. H. 2014, *ApJ*, 788, 43
- Usmanov, A. V. et al. 2016, *ApJ*, 820, 17
- Usmanov, A. V., Matthaeus, W. H., Goldstein, M. L., & Chhiber, R. 2018, *ApJ*, 865, 25
- Vasquez, B. J., Smith, C. W., Hamilton, K., MacBride, B. T., & Leamon, R. J. 2007, *J. Geophys. Res.*, 112, A07101
- Wilcox, J. M, Hoeksema, J. T., & Scherrer, P. H. 1980, *Science*, 209, 603
- Williams, L. L., & Zank, G. P. 1994, *JGR*, 99, 19229
- Zank G. P., Matthaeus W. H. and Smith C. W. 1996 *JGR* 101 17093
- Zank, G. P., Matthaeus, W. H., & Smith, C. W. 1996, *J. Geophys. Res.*, 101, 17,093-17,107
- Zank, G. P., Dosch, A., Hunana, P., Florinski, V., Matthaeus, W. H., & Webb, G. M. 2012, *ApJ*, 745, 35
- Zank, G. P., Adhikari, L., Hunana, P., Shiota, D., Bruno, R., & Telloni, D. 2017, *ApJ*, 835, 147
- Zank, G. P. 1999, *Space Sci. Rev.*, 89, 413–688
- Zank, G. P. 2016 *Geosci. Lett.* 3, 22
- Zhou, Y., & Matthaeus, W. H. 1990a, *J. Geophys. Res.*, 95, 10291-10311
- Zhou, Y., & Matthaeus, W. H. 1990b, *J. Geophys. Res.*, 95, 14,881-14,892

Curriculum Vitae

Education

University of New Hampshire, B.S. in Physics with Dual Major in Russian, May 2023

Skills and Relevant Coursework

MATLAB, Python, LaTeX, Microsoft & Google Suite. Russian Language B2 (Advanced) level. Certified Radiation Worker.

Quantum Mechanics I & II, Electricity and Magnetism I & II, Space Plasma Physics, General Relativity and Cosmology, Experimental Physics Lab I & II.

Publications, Presentations, Contributions

Anastasia V. Marchuk et al. "Low-frequency Waves due to Newborn Interstellar Pickup He⁺ Observed by the Ulysses Spacecraft" 2021 ApJ 923 185

Abigale S. Watson et al. "High-latitude Observations of Inertial-range Turbulence by the Ulysses Spacecraft During the Solar Minimum of 1993–96" 2022 ApJ 927 43 (coauthor)

Marchuk et al. "Low-frequency Waves due to Newborn Interstellar Pickup He⁺ Observed by the Ulysses Spacecraft" (2022) – Presented at the Annual Community Workshop of the Center for Geospace Storms, John Hopkins University

Marchuk, Anastasia V. and Smith, Charles, "Low-frequency Waves due to Newborn Interstellar Pickup He⁺ Observed by the Ulysses Spacecraft" (2022) – presented at the UNH Undergraduate Research Conference

Marchuk et al. SH014-10 (Presenter at American Geophysical Union Annual Meeting in 2020: Tuesday PM 12/8/20)

Watson et al. SH020-07 (Contributor to presentation American Geophysical Union Annual Meeting in 2020: Wednesday PM 12/9/20)

Experience

Undergraduate Student Researcher

6/18 - Present

University of New Hampshire, Durham, NH

- Developed a data base of Ulysses observations that includes waves excited by newborn interstellar pickup ions and heliospheric turbulence - Marchuk et. al (2021) describes findings of low frequency waves due to He⁺ pickup ions
- Built and deployed fluxgate magnetometers as part of a ground-based network across northern New England known as the Space Weather UnderGround (SWUG)

- Wrote documentation for the data logger used in the magnetometer deployment, explaining the build process and software upload
- Currently analyzing the database of Ulysses observations and proton temperature data to investigate high frequency events, and learning Drupal to develop a SWUG website

Website Developer

2/23 - Present

University of New Hampshire, Durham, NH

- Developed WordPress website from scratch as part of a project to expand common knowledge of the history of scientific development and discoveries, and give credit to non-Western scientists, mathematicians, and thinkers who are often overlooked
- Ongoing website maintenance, upkeep, and further development as the project continues

Club President

22-23 Season

UNH Fencing Team, Durham, NH

- Managed a full fencing team with 3 squads, one for each weapon, and worked with the executive board to create practice plans and goals
- Arranged transportation to tournaments, equipment purchase and repair, managed the team's equipment loan system, and set up fundraisers to cover team expenses
- Organized the annual UNH Invitational tournament, including hiring referees, acquiring event space, inviting schools, and managing setup and breakdown of equipment
- Applied for several grants to fund purchase of new equipment, tournament entry fees, and travel costs to our national conference championship
- When the team was faced with losing practice space and time slot, successfully advocated for the interests of our team and two other sport clubs to the recreation center staff

Figure Skating Coach

9/17 - Present

Great Bay Figure Skating Club, Dover, NH

- Teaching children and adults at all levels of ability basic to advanced figure skating or hockey skills
- Developed strategies to explain concepts to students in an understandable way, with ages ranging from 3 years old to adult. SafeSport Certified, US Figure Skating (USFS) compliant Learn to Skate and private coach

Achievements

- 2023 Recipient of Stanley A. Hamel Traveling Fellowship
- Inducted into Sigma Pi Sigma, AIP's Physics and Astronomy Honors Society (2022)
- Hamel Scholar, University of New Hampshire

- Presidential Scholarship, University of New Hampshire
- Selected for Gilman Scholarship (cancelled due to COVID)
- USFS Gold Medalist - Moves in the Field, 2017
- USFS Gold Medalist - Free Skate with Distinction, 2018

Activities

Undergraduate Curriculum Committee, Dept. of Physics and Astronomy (2021-22)

Society of Physics Students, University of New Hampshire

Figure Skater, Great Bay Figure Skating Club, Ice Skating Club of Exeter

Fencer (foil), UNH Fencing Team